\*\*Volume Title\*\*
ASP Conference Series, Vol. \*\*Volume Number\*\*
\*\*Author\*\*

© \*\*Copyright Year\*\* Astronomical Society of the Pacific

# On the seismic scaling relations $\Delta v - \bar{\rho}$ and $v_{\text{max}} - v_{\text{c}}$

K. Belkacem<sup>1</sup>, R. Samadi<sup>1</sup>, B. Mosser<sup>1</sup>, M.J. Goupil<sup>1</sup> and H.-G. Ludwig<sup>2,3</sup>

<sup>1</sup>LESIA, UMR8109, Observatoire de Paris, Université Pierre et Marie Curie, Université Denis Diderot, 92195 Meudon Cedex, France.

<sup>2</sup>Zentrum für Astronomie der Universität Heidelberg, Landessternwarte, Königstuhl 12, D-69117 Heidelberg, Germany

<sup>3</sup>GEPI, Observatoire de Paris, CNRS UMR 8111, Université Denis Diderot, 5 Place Jules Janssen, 92195 Meudon Cedex, France

**Abstract.** Scaling relations between asteroseismic quantities and stellar parameters are essential tools for studying stellar structure and evolution. We will address two of them, namely, the relation between the large frequency separation  $(\Delta \nu)$  and the mean density  $(\bar{\rho})$  as well as the relation between the frequency of the maximum in the power spectrum of solar-like oscillations  $(\nu_{max})$  and the cut-off frequency  $(\nu_c)$ .

For the first relation, we will consider the possible sources of uncertainties and explore them with the help of a grid of stellar models. For the second one, we will show that the basic physical picture is understood and that departure from the observed relation arises from the complexity of non-adiabatic processes involving time-dependent treatment of convection. This will be further discussed on the basis of a set of 3D hydrodynamical simulation of surface convection.

# 1. Introduction

The advent of space-borne asteroseismology has been possible with the space missions CoRoT (Baglin et al. 2006a,b; Michel et al. 2008) and *Kepler* (Borucki et al. 2010). These two missions have provided a wealth of high-quality and long-duration observational data that enable us to measure and characterize stellar oscillations. Among others, stars pulsating with solar-like oscillations (*i.e.* excited and damped by the uppermost convective layers of low-mass stars) are particularly important since they show a rich spectrum allowing for a probe of their internal structure (e.g. Goupil et al. 2011b,a; Christensen-Dalsgaard 2012).

Up to now, several hundreds of main-sequence stars with solar-like oscillations have been detected, as well as several thousands oscillating red giant stars. These observation permit statistical analysis and gave birth to the *ensemble asteroseismology*. This new approach is allowed by the large-scale exploitation of *seismic indices* that are also called global seismic parameters. As depicted in Fig. 1, one can easily identify two major seismic indices, namely:

• the large separation,  $\Delta v \equiv \langle v_{n+1,\ell} - v_{n,\ell} \rangle$  (where  $v_{n+1,\ell}$  is the frequency, n is the radial order,  $\ell$  is the angular degree, and  $\langle \cdot \rangle$  stands for an average over frequency.).

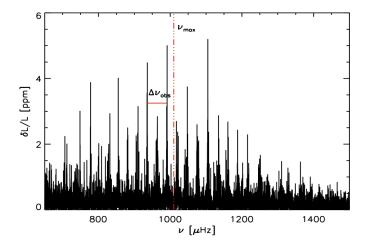


Figure 1. Power spectrum as a function of frequency of the star HD49385 observed by CoRoT during a period of 137 days (see Deheuvels & Michel 2011, for details). The vertical red dotted-dashed line represents the position of  $\nu_{\rm max}$  while the red solid horizontal segment illustrates the large separation ( $\Delta\nu_{\rm obs}$ ) between two modes of same angular degree.

• the frequency of the maximum height in the power spectrum,  $v_{\text{max}}$ , which is defined such as  $H(v_{\text{max}}) = max[H(v)]$ , where H is the height in the power spectrum corrected from the background<sup>1</sup>.

Although other scaling relations are available, we will restrict our focus to these quantities in this article.

The determination of seismic indices provides a wealth of information since they can be related to global stellar parameters through *scaling relations*. One can define them as relations between seismic indices and global stellar parameters such as the mass, radius, or effective temperature. The two commonly used relations are (e.g., Ulrich 1986; Brown et al. 1991; Kjeldsen & Bedding 1995; Belkacem et al. 2011):

• the relation between  $\Delta \nu$  and the squared mean density of the star, *i.e.* 

$$\Delta \nu \propto \bar{\rho}^{1/2} \equiv \left(\frac{3}{4\pi} \frac{M}{R^3}\right)^{1/2} \,, \tag{1}$$

where  $\bar{\rho}$  is the mean density, M is the total mass of the star, and R is total radius.

• The second one relates the frequency of the maximum height in the power spectrum to the cut-off frequency, *i.e.* 

$$v_{\rm max} \propto v_{\rm c} \propto \frac{g}{\sqrt{T_{\rm eff}}} \propto \frac{M}{R^2 \sqrt{T_{\rm eff}}},$$
 (2)

<sup>&</sup>lt;sup>1</sup>We note that alternative definitions of  $v_{\text{max}}$  are possible and in particular in terms of mode amplitude rather than mode height (see Belkacem 2012, for a discussion), but for consistency with the theoretical results of Belkacem et al. (2011) we adopt this definition.

where  $v_c$  refers to the cut-off frequency, *i.e.* the frequency above which there is no more total reflection at the star surface.

From Eq. (1) and Eq. (2), the potential of ensemble asteroseismology immediately arises because one can derive an estimate of stellar masses and radii (or alternatively mean densities and surface gravities) provided a determination of the effective temperature is available

$$\frac{M}{M_{\odot}} \propto \left(\frac{v_{\text{max}}}{v_{\text{max}}^{\odot}}\right)^{3} \left(\frac{\Delta v}{\Delta v_{\odot}}\right)^{-4} \left(\frac{T_{\text{eff}}}{T_{\text{eff},\odot}}\right)^{3/2},$$
 (3)

$$\frac{R}{R_{\odot}} \propto \left(\frac{\nu_{\text{max}}}{\nu_{\text{max}}^{\odot}}\right) \left(\frac{\Delta \nu}{\Delta \nu_{\odot}}\right)^{-2} \left(\frac{T_{\text{eff}}}{T_{\text{eff},\odot}}\right)^{1/2},$$
 (4)

where  $T_{\rm eff}$  is the effective temperature, and the symbol  $\odot$  denotes the solar reference values. Equations (3) and (4) are the cornerstones of ensemble asteroseismology and provide a wealth of constraints on stellar structure and evolution, as well as stellar populations (see Chaplin & Miglio 2013, for a recent review).

In this article, our objective is to investigate the physical foundations of this scaling relations. Indeed, many efforts are currently being undertaken to calibrate and validate these relations (e.g. Bedding 2011; Bruntt et al. 2011; Miglio 2012; Huber et al. 2012; Silva Aguirre et al. 2012) but a firm theoretical ground is certainly the best way to ensure their proper and well-motivated use. Such theoretical investigations have been previously performed (e.g. Stello et al. 2009; White et al. 2011; Belkacem et al. 2011; Montalbán et al. 2012; Miglio et al. 2012; Montalbán & Noels 2013), but there is still a large gap to fill to reach a full and satisfying understanding. We will therefore discuss the fundamental physical concept underlying the scaling relations presented in Eqs. (3) and (4). In Sect. 2, we address the  $\Delta v - \bar{\rho}$  relations and, with the help of stellar modeling, we discuss the accuracy of this relation. Section 3 will be dedicated to the  $v_{\text{max}} - v_{\text{c}}$  scaling relation by discussing its theoretical background with the help of a set of 3D hydrodynamical simulations. Finally, concluding remarks are provided in Sect. 4.

## 2. The $\Delta v - \bar{\rho}$ scaling relation

In this section, we discuss the possible sources of departure from the  $\Delta v - \bar{\rho}$  relation. But before going through the details, it is worth to make clear some definitions, summarized in Fig. 2.

# 2.1. Preliminary definitions

From an observational point of view, the *observed* large separation is the near regularity measured around  $\nu = \nu_{\rm max}$  because it is obviously the frequency for which the signal-to-noise ratio is maximum. It corresponds to radial order of about 20 for main-sequence stars down to two near the tip of the red giant branch. Indeed, as a low-mass star evolves, it exhibits excited solar-like oscillations at lower radial orders. We therefore define the large separation measured near  $\nu_{\rm max}$  as  $\Delta\nu_{\rm obs}$  (see Mosser et al. 2013b, for a more detailed discussion on  $\Delta\nu_{\rm obs}$ ). Note that, in this article,  $\Delta\nu_{\rm obs}$  is obtained by using computed frequencies as a proxy of measured frequencies.

On the other hand, from a theoretical point of view, the large separation is a quantity introduced from an asymptotic analysis (e.g. Tassoul 1980; Gough 1990) and as

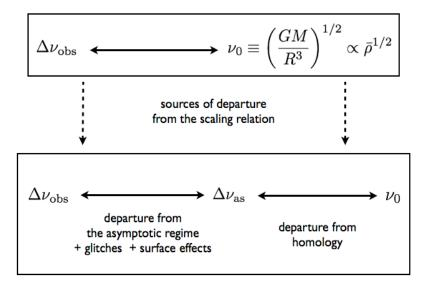


Figure 2. Sketch that illustrates the relation between the large separation and the mean density (top panel). The possible sources of departure from the scaling relation are displayed in the bottom panel, with particular emphasis on the intermediate quantity  $\Delta v_{\rm as}$  (defined in Sect. 2.1).

such it is formally valid at high radial orders. In other words, the requirements is that the characteristic vertical wavelength of the eigenfunctions must be small compared to the scale of variation of the equilibrium state (i.e.  $k_r H_{\{p,\rho,T\}} \gg 1$ , where  $k_r$  is the radial wavenumber of the oscillation,  $H_{\{p,\rho,T\}}$  are the pressure, density, and temperature scale heights, respectively). Under this assumption, the large separation becomes

$$\Delta v_{\rm as} \equiv \left(2 \int_0^R \frac{\mathrm{d}r}{c_s}\right)^{-1} = (2\tau)^{-1},\tag{5}$$

where  $c_s$  is the adiabatic sound speed, and the quantity  $\tau$  is the acoustic radius. Except the aforementioned large separations, one can also define  $\nu_0$  such as

$$\nu_0 \equiv \left(\frac{GM}{R^3}\right)^{1/2} \propto \bar{\rho}^{1/2} \,. \tag{6}$$

This quantity is the inverse of the dynamical time-scale of a star, and as such can be called the dynamical frequency. It is then related to the mean density  $(\bar{\rho})$ .

# 2.2. Theoretical background of the $\Delta v_{as} - v_0$ relation: homology

As displayed in Fig. 2, the relation between  $\Delta \nu_{\rm obs}$  and  $\nu_0$  can be decomposed to introduce, as an intermediate, the quantity  $\Delta \nu_{\rm as}$ . Such a decomposition is useful since it makes clear the possible sources of departure from a perfect scaling (see Sect. 2.3). It leads to identify that the main physical assumption is the homology between  $\Delta \nu_{\rm as}$  and  $\nu_0$ .

Let us consider two homologous stars, such that for two shells verifying r/R = r'/R', the corresponding mass shells are equal (m/M = m'/M'), where M, M' are the

total masses of two stars belonging to a homologous series, and R, R' their total radii. Under this assumption, it is possible to show from the equations of mass continuity and conservation of momentum that the sound speeds of both models are related by (see for instance Sect. 20.1 of Kippenhahn & Weigert 1990)

$$\frac{c_s}{c_s'} = \left(\frac{M}{M'}\right)^{1/2} \left(\frac{R}{R'}\right)^{-1/2} . \tag{7}$$

Using Eq. (7) together with the relation r/R = r'/R', it is straightforward to demonstrate the desired scaling relation, *i.e.* 

$$\frac{\Delta \nu_{\rm as}}{\Delta \nu_{\rm as}'} = \left[ \int_0^{R'} \frac{\mathrm{d}r'}{c_s'} \right] \left[ \int_0^R \frac{\mathrm{d}r}{c_s} \right]^{-1} = \left( \frac{R'}{R} \right)^{3/2} \left( \frac{M}{M'} \right)^{1/2} . \tag{8}$$

In other words, if one of the considered star is the Sun, one has

$$\Delta \nu_{\rm as} = \left(\frac{\bar{\rho}}{\bar{\rho}_{\odot}}\right)^{1/2} \Delta \nu_{\odot,\rm as} , \qquad (9)$$

Equation (9) demonstrates the scaling relation between  $\Delta \nu_{as}$  and  $\bar{\rho}$ , and shows that the underlying hypothesis is homology. This assumption is in general considered as a crude one, which is however useful to get some insight into more complex models obtained from a full numerical computation. As discussed extensively for instance by Kippenhahn & Weigert (1990), the main physical requirements for complete homology to holds are

- Complete equilibrium, *i.e.* that both stars must be in both hydrostatic and thermal equilibrium.
- The mean Rosseland opacities, the equation of state, and the energy generation rate must be power laws of density and temperature (or equivalently pressure and temperature).
- The physical mechanism that transports energy (convection or radiation) must be the same in the considered stars.

When applying the  $\Delta \nu_{as} - \nu_0$  relation between two low-mass stars from the mainsequence to the red giant branch as well as the red clump, all those requirements are violated. Nevertheless, one must keep in mind that mainly the upper layers will contribute to  $\Delta \nu_{as}$  since the inverse of the sound speed is higher in those layers (see Eq. 5). Therefore, the consequences of the violation of the aforementioned requirements are not obvious, and as we will show and quantify in Sect. 2.3, the  $\Delta \nu_{as} - \nu_0$  relation is quite accurate.

#### 2.3. Sources of departure from the scaling relation

As depicted in Fig. 2, to infer the sources of uncertainties of the  $\Delta \nu_{\rm obs} - \nu_0$ , it is useful to consider separately the  $\Delta \nu_{\rm obs} - \Delta \nu_{\rm as}$  and  $\Delta \nu_{\rm as} - \nu_0$  relations. We therefore quantified, with the help of a grid of stellar models, the departure from a 1:1 scaling of both relations.

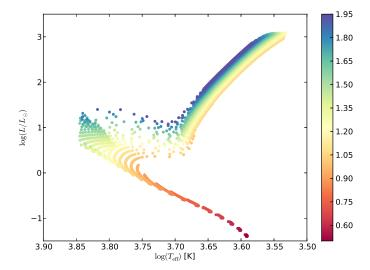


Figure 3. Position of the stellar modes in the Hertzsprung-Russell diagram. The color of the symbols correspond to masses in solar units of the models, and the corresponding color scale is given in the vertical color bar.

#### 2.3.1. Grid of stellar models

The grid was computed with the CESTAM code (Marques et al. 2013) and includes stellar models with masses ranging from  $M=0.5~M_{\odot}$  to  $M=1.95~M_{\odot}$  (see Fig. 3). The models include standard physics and do not include microscopic diffusion nor rotation. They all have a solar metal abundance assuming Asplund et al. (2005) chemical mixture (i.e. Y=0.2485 and Z/X=0.165). The positions of the models in the Hertzsprung-Russell diagram are shown Fig. 3. The theoretical mode frequencies associated with the stellar models are obtained with the ADIPLS code (Christensen-Dalsgaard 2011). The stellar models were re-meshed with an adapted grid of 8 000 points. We consider only radial order modes. For each stellar model, radial eigenfrequencies are used to compute  $\Delta \nu_{\rm obs}$ . For  $\Delta \nu_{\rm obs}$  we proceed in practice in a similar way as White et al. (2011), *i.e.* we determine  $\Delta \nu_{\rm obs}$  by adjusting by means of least-square the first-order asymptotic relation

$$\nu_{n,0} = \Delta \nu_{\text{obs}} (n + \epsilon) , \qquad (10)$$

where  $v_{n,0}$  is the radial mode eigenfrequency, n the associated radial order, and  $\epsilon$  an offset. The weight entering the least square fit is a Gaussian function centered on  $v_{\text{max}}$ . The FWHM of the Gaussian function,  $\delta v_{\text{env}}$  is assumed to depend on  $v_{\text{max}}$ . For stars with  $v_{\text{max}} < 200 \, \mu\text{Hz}$  (RG stars), we adopt the scaling relation obtained by Mosser et al. (2012), while above  $v_{\text{max}} = 200 \, \mu\text{Hz}$ ,  $\delta v_{\text{env}}$  is assumed to scale linearly with  $v_{\text{max}}$ .

#### **2.3.2.** The $\Delta v_{\rm obs} - \Delta v_{\rm as}$ relation

Let us first consider the intermediate relation between  $\Delta \nu_{\rm obs}$  and  $\Delta \nu_{\rm as}$ . As shown by Fig. 4 (top panel), the departure from unity of the ratio  $\Delta \nu_{\rm obs}/\Delta \nu_{\rm as}$  is of several percent for main-sequence stars and early sub-giant and can reach up to 15 % for red giant stars

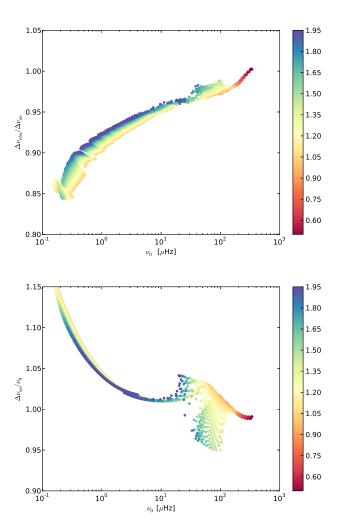


Figure 4. **Top:**  $(\Delta \nu_{obs}/\Delta \nu_{as})$  as a function of  $\nu_0$  for stellar models as described in Sect. 2.3.1 and summarized in the HR diagram (Fig. 3). Same color code as in Fig. 3. **Bottom:** The same as for the top panel but for the ratio  $(\Delta \nu_{as}/\nu_0)$ .

near the tip of the branch. We also note that the dispersion remains small. Therefore, this departure is only weakly mass dependent.

There are several physical reasons that can explain such a departure from a perfect scaling, namely: the departure from the asymptotic expansion (*i.e.* the conditions  $n \gg 1$  is not fulfilled), glitches (*i.e.* the effect of discontinuities of the sound speed profile), or surface effects (*e.g.* effects of turbulent pressure and non-adiabatic processes that are not considered in the computations).

Among all those possible biases, the departure from the asymptotic regime seems the dominant one for red giant stars. Indeed, while  $n_{\rm max} \simeq 20$  for main-sequence stars, it decreases as the stars evolve on the subgiant and red giant phases to reach up to  $n_{\rm max} \simeq 2$  near the tip of the branch. A correction of this effects has recently been proposed by Mosser et al. (2013b) (see also Hekker et al. 2013). It provides an estimate of the bias between  $\Delta \nu_{\rm obs}$  and  $\Delta \nu_{\rm as}$ , which is in qualitative agreement with Fig. 4 (top panel).

More insights are nevertheless desirable to fully understand the departures between  $\Delta v_{\rm obs}$  and  $\Delta v_{\rm as}$ . This will need to investigate the effects of varying the input physics of the models and this should help to fine-tune prescriptions (such as proposed by Mosser et al. 2013b) to relate  $\Delta v_{\rm obs}$  and  $\Delta v_{\rm as}$ .

#### **2.3.3.** The $\Delta v_{\rm as} - v_0$ relation

The ratio  $\Delta v_{\rm as}/v_0$  as a function of  $v_0$  is displayed in Fig. 4 (bottom panel). One immediately sees that the departure from a perfect scaling is up to 5 % for main-sequence stars, with an important dispersion in mass, and can reach up to 10 % for red-giant stars, but with a small dispersion in mass.

From a physical point of view, these behaviors can be understood on the basis of the homology as already presented in Sect. 2.2. For main-sequence stars,  $\Delta v_{as}$  remains sensitive to the physical conditions in the core. This explains the dispersion in mass that reflects the variations of the physical conditions along the main-sequence phase with the mass. For instance, as the mass increases, the nuclear reactions switch from a p-p chain to a CNO chain (inducing a change in the mechanism of transport of energy from a radiative to a convective transport in the core). This of course violates the conditions for homology to apply, as discussed in Sect. 2.2.

For sub-giant stars and giant stars the situation is quite different. Indeed, as the star evolves, its core contracts and its envelope dilates, so that the integral involved in the computation of  $\Delta v_{\rm as}$  mainly depends on the convective upper layers. Adiabatic convection is reasonably well modeled by a polytrope of index 1.5 and it is well known that two polytropes of same index are homologous (e.g., Chandrasekhar 1967). Consequently, one can infer that the departure of a ratio  $\Delta v_{\rm as}/v_0$  from unity and its trend are dominated by the increasing influence of the super-adiabatic layers as a star evolves.

Once again, a more dedicated work on this issue will help to improve the accuracy of the  $\Delta v_{as} - v_0$  relation.

#### 2.4. Discussion

Finally, the departure of  $\Delta \nu_{\rm obs}$  from  $\nu_0$  shown in Fig. 5 is up to 5%, with a strong dependence on mass for main-sequence stars and sub-giants stars, while for RGB stars with  $\nu_0 \lesssim 600\,\mu{\rm Hz}$ , this departure depends more weakly on the mass and – in average – slowly increases with decreasing  $\nu_0$ . It is striking to note that there is a smaller departure of  $\Delta \nu_{\rm obs}$  from  $\nu_0$ , which is mainly explained by the compensation effect of the departure

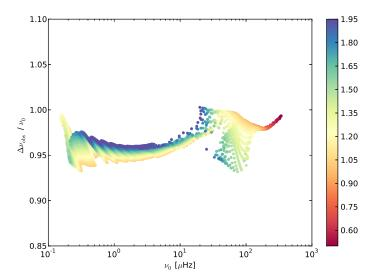


Figure 5. Ratio  $\Delta v_{\rm obs}/v_0$  as a function of  $v_0$  (see Sect. 2.1 for the definitions). The grid of models is the same as in Fig. 3. Same color code as in Fig. 3.

of the mode frequencies from the asymptotic regime (*i.e.* from the  $\Delta v_{\rm obs} - \Delta v_{\rm as}$  relation) with the departure from the homology (*i.e.* from the  $\Delta v_{\rm as} - v_0$  relation).

Whether this is a coincidence or can be explained by some fundamental reasons remains an open issue. Anyway, it is quite a good news since it justifies the extensive use of the  $\Delta\nu_{\rm obs} - \nu_0$  scaling relation. Moreover, it allows the use of  $\Delta\nu_{\rm obs}$  to derive stellar parameters and more particularly for red-giant stars, for obtaining a proxi of the stellar mass and radius.

## 3. The $v_{\text{max}} - v_{\text{c}}$ scaling relation

As introduced in Sect. 1, the scaling relation that provides an estimate of the surface gravity derives from the proportionality between  $\nu_{\rm max}$  and  $\nu_{\rm c}$ . In this section, we discuss the theoretical foundations of this scaling relation. We follow the work of Belkacem et al. (2011), which shows that this relation can be explained by two intermediate relations, namely  $\nu_{\rm max} - \tau_{\rm th}^{-1}$  (where  $\tau_{\rm th}^{-1}$  is the thermal frequency, see Sect. 3.2 for a precise definition) and the  $\tau_{\rm th}^{-1} - \nu_{\rm c}$ , as displayed in Fig. 6.

# 3.1. The transition region and the $v_{max}$ – $v_{th}$ relation

The frequency  $v_{\text{max}}$  is determined by the maximum height H of the background-corrected power spectrum. For stochastically excited modes, the height of the mode profile in the power spectrum is given by (e.g. Libbrecht 1988; Chaplin et al. 1998; Baudin et al. 2005; Chaplin et al. 2005; Belkacem et al. 2006)

$$H = \frac{P}{2\eta^2 \mathcal{M}}, \quad \text{with} \quad \mathcal{M} = \int_0^M \frac{|\xi|^2}{|\xi(M)|^2} dm, \qquad (11)$$

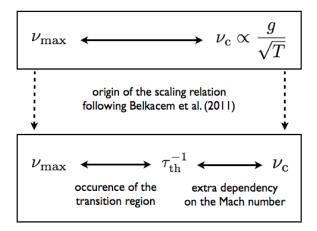


Figure 6. Sketch that illustrates the relation between  $v_{\text{max}}$  and  $v_{\text{c}}$  (top panel). Following the work of Belkacem et al. (2011), the bottom panel explicits the intermediate frequency that is the thermal frequency.

where P is the excitation rate,  $\eta$  is the damping rate,  $\mathcal{M}$  is the mode mass, and  $\xi$  is the mode displacement. As shown for instance by Chaplin et al. (2008); Belkacem et al. (2011), and confirmed with observations of the solar-like stars by *Kepler* (Appourchaux et al. 2012), the maximum of H is predominantly determined by the squared damping rates ( $\eta^2$ ) in Eq. (11). More precisely,  $\nu_{\text{max}}$  arises from the depression (or plateau) of  $\eta$ .

The depression of the damping rates occurs when the modal period nearly equals the thermal time-scale (or thermal adjustment time-scale) in the superadiabatic layers. This was first mentioned by Balmforth (1992) (see his Sect. 7.2 and 7.3) and confirmed by Belkacem et al. (2011), on the basis of two different non-adiabatic pulsation codes. In the context of classical pulsators, the location of this equality is referred to as the transition region (e.g. Cox 1974, 1980) and its occurrence in the ionization region is one of the necessary condition for a mode to be excited by the  $\kappa$ -mechanism (e.g., Cox 1980; Cox & Giuli 1968; Pamyatnykh 1999). In the context of solar-like pulsators, the situation is very similar, except that the destabilization by the perturbation of the opacity never dominates over damping terms (Belkacem et al. 2012) and that the situation is complicated by the presence of convection which modifies the thermal time-scale (see Belkacem et al. 2011; Belkacem 2012, for details). This is illustrated in Fig. 7, which displays the mode damping rates computed using the Grigahcène et al. (2005) formalism. It confirms that the perturbation of the opacity is the corner-stone of the relation between the modal period and the thermal time-scale.

#### 3.2. The $v_{th} - v_c$ relation from 3D numerical simulations

As shown in the previous section, there is a linear relation between  $\nu_{max}$  and the thermal frequency  $\nu_{th} \equiv \tau_{th}^{-1}$ . Let us now investigate the relation between  $\nu_{th}$  and  $\nu_{c}$ .

The thermal adjustment time-scale has been extensively discussed by Cox & Giuli (1968); Cox (1980); Pesnell (1983). It is defined as

$$\tau_{\rm th} = \frac{1}{L} \int_{m_{\rm tr}}^{M} c_{\nu} T \, \mathrm{d}m \tag{12}$$

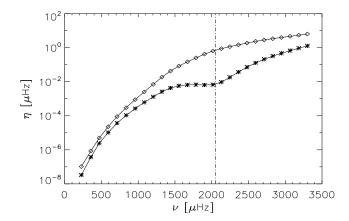


Figure 7. Mode damping rates versus mode frequency computed for a model of one solar mass on the main-sequence, using the Grigahcène et al. (2005) formalism as described in Belkacem et al. (2012). The star symbols correspond to the full computation while the diamond symbols correspond to the computation for which we imposed  $\delta\kappa/\kappa=0$ . The vertical dashed-dotted line corresponds to the frequency  $\nu_{\rm max}$  computed using the scaling relation (Eq. 2).

where M is the total mass,  $c_v$  is specific heat capacity at fixed volume, and  $m_{\rm tr}$  is the mass at the transition region. As already explained in Sect. 3.1, the relation between  $v_{\rm max}$  and  $v_{\rm th}$  holds due to the occurrence of the transition region in the ionization region. Accordingly, we compute lower boundary of the integral in Eq. (12) as the minimum of  $(\Gamma_3 - 1) = (\partial \ln T/\partial \ln \rho)_s$ , where s is the specific entropy<sup>2</sup>.

For the cut-off frequency, a general expression has been proposed by Balmforth & Gough (1990)

$$\omega_c = 2\pi \nu_c = \left(\frac{c_s}{2H_\rho}\right) \sqrt{1 - 2\frac{\mathrm{d}H_\rho}{\mathrm{d}r}} \tag{13}$$

with  $c_s$  the sound speed, and  $H_\rho = -(\mathrm{d} \ln \rho/\mathrm{d} r)^{-1}$  the density scale height. For an isothermal atmosphere,  $\omega_c$  reduces to

$$\omega_c = \frac{c_s}{2H_o} \,. \tag{14}$$

To go further it is customary to use the pressure scale height  $(H_p)$  as a proxy for the density scale height. This is based on the fact that both quantities are nearly equal at the photosphere. Finally, it can be shown that  $H_p$  scales as the ratio between the surface gravity and the square root of the effective temperature. Consequently, in the following, we will denote and compute the cut-off frequency as

$$\omega_c = \frac{c_s}{2H_p} \propto \frac{g}{\sqrt{T_{\text{eff}}}},\tag{15}$$

where we considered all the quantities at the photosphere, and we made use of the scaling relations  $c_s^2 \propto T_{\rm eff}$ ,  $H_p \propto T_{\rm eff}/g$ .

<sup>&</sup>lt;sup>2</sup>Note that the scaling is hardly sensitive to this lower boundary.

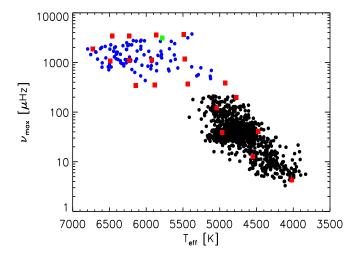


Figure 8.  $v_{\rm max}$  as a function of the effective temperature ( $T_{\rm eff}$ ). The filled red squares corresponds to the location of the 3D hydrodynamical models (see text for details), the filled blue circles to sub-giant and main-sequence targets observed by *Kepler* (Chaplin et al. 2011), and the black ones to the red-giant stars observed by *Kepler* (Mathur et al. 2011). Finally, the green square corresponds to the solar 3D model.

Belkacem et al. (2011) used the mixing-length formalism to derive a linear relation between  $v_{th}$  and  $v_c$ . However, it is well-known that the MLT suffers many deficiencies and particularly near the photosphere. Therefore, we propose here to employ a set of 3D hydrodynamical numerical simulations. To this end, we used 3D models from the CIFIST grid (Ludwig et al. 2009). The CIFIST grid covers the main sequence and the giant branch of late-type stars. All 3D models used here have a solar metal abundance with a chemical mixture similar to the solar chemical composition proposed by Asplund et al. (2005). Their characteristics are extensively described in Samadi et al. (2013). We determine for each 3D model the associated radius using a grid of standard stellar models computed with the CESTAM code (Marques et al. 2013). The stellar 1D models have the same chemical composition than the 3D models.

Figure 8 shows how the selected simulations span into the  $\log g - T_{\rm eff}$  (which translates in the  $\nu_{\rm max} - T_{\rm eff}$  from an observational point of view) diagram and how it compares with the recent *Kepler* and CoRoT observations. Our 3D models are representative of the current observations of solar-like pulsators from the main-sequence to the red-giant phase. The linear relation derived by Belkacem et al. (2011) is confirmed by the 3D models, even if there is some dispersion especially for main-sequence stars (see the top panel of Fig. 9). In addition, we confirm that the main source of uncertainty is related to an extra factor that is the Mach number ( $\mathcal{M}_a$ ). More precisely, let us assume that

$$\tau_{\rm th}^{-1} \propto \mathcal{M}_a^{\alpha} \, \nu_{\rm c} \,, \tag{16}$$

so that one can derive  $\alpha$  to minimize the dispersion. It gives

$$\alpha = 2.78 \tag{17}$$

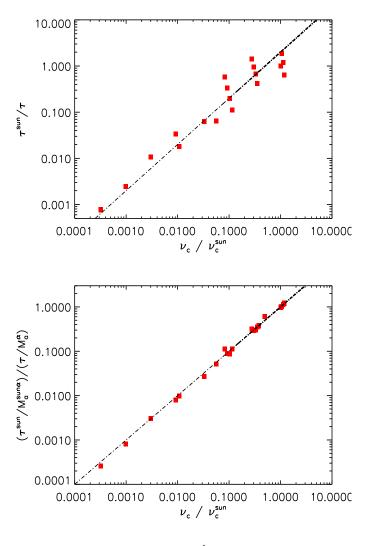


Figure 9. *Top panel:* Thermal frequency  $\tau_{th}^{-1}$  as a function of the cut-off frequency  $\nu_c$ . All the quantities are normalized by the values derived from the Solar 3D simulation. The filled squared correspond to the 3D models displayed in Fig. 8. The dashed-dotted line corresponds to the linear curve. *Bottom panel:* As for the top panel, except that the thermal frequency is corrected by the term  $\mathcal{M}_a^{\alpha}$  with  $\alpha = 2.78$  (see Eq. (16)).

This result agrees with what can be derived from the mixing length theory, *i.e.*  $\alpha = 3$ . Indeed, this is quite a robust number since the dependence to the Mach number can be derived from simple energetical arguments that hardly depend on the assumptions related to the MLT. The resulting scaling relation, that accounts for the dependence on the Mach number, is depicted in Fig. 9 (bottom panel). It confirms that most of the dispersion of the  $v_{\text{th}} - v_{\text{c}}$  relation (and therefore the  $v_{\text{max}} - v_{\text{c}}$  relation) comes from the extra dependence on  $\mathcal{M}_a$ . Note that further investigations on the influence of the Péclet number (ratio of the radiative to the convective time-scales) would be desirable (see Tremblay et al. 2013).

## 3.3. Effect of the Mach number on the scaling for stars on the red giant branch

In this section, our objective is to investigate why the effect of the Mach number seems to be negligible on the  $\nu_{max} - \nu_{c}$  relation for red-giant stars, as shown in Fig. 9 (top panel). To this end, we will first make several assumptions that will enable us to derive a scaling between the Mach number and stellar global parameters. First we assume that the total flux is convective and proportional to the kinetic energy flux, so that

$$\mathcal{M}_a \propto T_{\text{eff}}^{5/6} \rho^{-1/3} \,,$$
 (18)

where  $\rho$  is the surface density. To go further, we note that the surface density does not scale as the mean density  $\bar{\rho}$ . We therefore use the fact that the optical depth is roughly  $\tau \simeq \kappa \rho H_p \equiv 2/3$  and that the opacity is dominated by H<sup>-</sup> so that  $\kappa \propto \rho^{1/2} T^9$  (e.g. Hansen & Kawaler 1994). Thus, Eq. (18) becomes

$$\mathcal{M}_a \propto T_{\text{eff}}^3 \, g^{-2/9} \,, \tag{19}$$

where *g* is the surface gravity.

As shown in Fig. 10, there is an additional relation between the surface gravity and the effective temperature of stars on the red giant branch. It reads

$$T_{\rm eff} \propto g^{0.07} \,. \tag{20}$$

This is in good agreement with the observations that give  $T_{\rm eff} \propto \nu_{\rm max}^{0.068}$  (Mosser et al. 2013a).

It is then possible to understand why the  $\nu_{max} - \nu_c$  relation hardly depends on the Mach number for red giant stars on the red giant branch. Indeed, the Mach number becomes nearly independent of both effective temperature and surface gravity. If we introduce Eq. (19) and Eq. (20) into Eq. (16), we obtain

$$\nu_{\rm max} \propto \mathcal{M}_a^3 \nu_{\rm c} \propto \frac{g^{0.988}}{\sqrt{T_{\rm eff}}} \approx {\rm cste} \times \nu_{\rm c} \,.$$
 (21)

This result shows that for red-giant stars near the tip of the branch, the effect of the Mach number becomes negligible. In other words, one can conclude that the  $\nu_{\text{max}} - \nu_{\text{c}}$  relation is more accurate for red giants since the possible biases introduced by the Mach number become small.

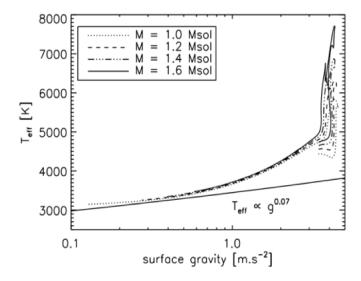


Figure 10. Diagram of the effective temperature versus surface gravity for models computed with the CESTAM code from the main-sequence to the red-giant branch.

#### 4. Concluding remarks

In this paper, we discussed the physical meaning of the scaling relations  $\Delta v - \bar{\rho}$  and  $v_{\text{max}} - v_{\text{c}}$ , the foundations of what is now commonly called *Ensemble Asteroseismology*.

We have discussed the  $\Delta v - \bar{\rho}$  relation with emphasis on the possible departure from a linear relation. It turns out that the relation holds within several percents from the main-sequence to the red giant phase. This validity is obtained thanks to compensating effects mainly between departure from the homology and from the asymptotic regime. Concerning the  $v_{\text{max}} - v_{\text{c}}$  relation, we confirm the physical interpretation of Belkacem et al. (2011) by using a set of of 3D hydrodynamic models representative for the CoRoT and *Kepler* observations.

Finally, one must note that, at this stage of our physical understanding of the  $\Delta \nu - \bar{\rho}$  and  $\nu_{\text{max}} - \nu_{\text{c}}$  scaling relations, it is not yet possible to firmly conclude about their accuracy.

**Acknowledgments.** K. B. is grateful to the organizers for their invitation and for providing financial support. HGL acknowledges financial support by the Sonderforschungsbereich SFB 881 "The Milky Way System" (subproject A4) of the German Research Foundation (DFG). We also acknowledge financial support from "Programme National de Physique Stellaire" (PNPS) of CNRS/INSU, France. The authors also acknowledge financial support from the French National Research Agency (ANR) for the project ANR IDEE (Influence Des Etoiles sur les Exoplanètes).

#### References

Appourchaux, T., Benomar, O., Gruberbauer, M., Chaplin, W. J., García, R. A., Handberg, R., Verner, G. A., Antia, H. M., Campante, T. L., Davies, G. R., Deheuvels, S., Hekker, S., Howe, R., Salabert, D., Bedding, T. R., White, T. R., Houdek, G., Silva Aguirre, V.,

- Elsworth, Y. P., van Cleve, J., Clarke, B. D., Hall, J. R., & Kjeldsen, H. 2012, A&A, 537, A134. 1112.3295
- Asplund, M., Grevesse, N., & Sauval, A. J. 2005, in Cosmic Abundances as Records of Stellar Evolution and Nucleosynthesis, edited by T. G. Barnes, III, & F. N. Bash, vol. 336 of Astronomical Society of the Pacific Conference Series, 25
- Baglin, A., Auvergne, M., Barge, P., Deleuil, M., Catala, C., Michel, E., Weiss, W., & COROT Team 2006a, in ESA Special Publication, edited by M. Fridlund, A. Baglin, J. Lochard, & L. Conroy, vol. 1306 of ESA Special Publication, 33
- Baglin, A., Auvergne, M., Boisnard, L., Lam-Trong, T., Barge, P., Catala, C., Deleuil, M., Michel, E., & Weiss, W. 2006b, in 36th COSPAR Scientific Assembly, vol. 36 of COSPAR Meeting, 3749

Balmforth, N. J. 1992, MNRAS, 255, 603

Balmforth, N. J., & Gough, D. O. 1990, ApJ, 362, 256

Baudin, F., Samadi, R., Goupil, M.-J., Appourchaux, T., Barban, C., Boumier, P., Chaplin, W. J., & Gouttebroze, P. 2005, A&A, 433, 349

Bedding, T. R. 2011, ArXiv e-prints. 1107.1723

Belkacem, K. 2012, in SF2A-2012: Proceedings of the Annual meeting of the French Society of Astronomy and Astrophysics, edited by S. Boissier, P. de Laverny, N. Nardetto, R. Samadi, D. Valls-Gabaud, & H. Wozniak, 173. 1210.3505

Belkacem, K., Dupret, M. A., Baudin, F., Appourchaux, T., Marques, J. P., & Samadi, R. 2012, A&A, 540, L7. 1203.1737

Belkacem, K., Goupil, M. J., Dupret, M. A., Samadi, R., Baudin, F., Noels, A., & Mosser, B. 2011, A&A, 530, A142. 1104.0630

Belkacem, K., Samadi, R., Goupil, M. J., Kupka, F., & Baudin, F. 2006, A&A, 460, 183. arXiv:astro-ph/0607570

Borucki, W. J., Koch, D., Basri, G., Batalha, N., Brown, T., Caldwell, D., Caldwell, J., Christensen-Dalsgaard, J., Cochran, W. D., DeVore, E., Dunham, E. W., Dupree, A. K., Gautier, T. N., Geary, J. C., Gilliland, R., Gould, A., Howell, S. B., Jenkins, J. M., Kondo, Y., Latham, D. W., Marcy, G. W., Meibom, S., Kjeldsen, H., Lissauer, J. J., Monet, D. G., Morrison, D., Sasselov, D., Tarter, J., Boss, A., Brownlee, D., Owen, T., Buzasi, D., Charbonneau, D., Doyle, L., Fortney, J., Ford, E. B., Holman, M. J., Seager, S., Steffen, J. H., Welsh, W. F., Rowe, J., Anderson, H., Buchhave, L., Ciardi, D., Walkowicz, L., Sherry, W., Horch, E., Isaacson, H., Everett, M. E., Fischer, D., Torres, G., Johnson, J. A., Endl, M., MacQueen, P., Bryson, S. T., Dotson, J., Haas, M., Kolodziejczak, J., Van Cleve, J., Chandrasekaran, H., Twicken, J. D., Quintana, E. V., Clarke, B. D., Allen, C., Li, J., Wu, H., Tenenbaum, P., Verner, E., Bruhweiler, F., Barnes, J., & Prsa, A. 2010, Science, 327, 977

Brown, T. M., Gilliland, R. L., Noyes, R. W., & Ramsey, L. W. 1991, ApJ, 368, 599

Bruntt, H., Frandsen, S., & Thygesen, A. O. 2011, A&A, 528, A121. 1012.0436

Chandrasekhar, S. 1967, An introduction to the study of stellar structure

Chaplin, W. J., Elsworth, Y., Isaak, G. R., Lines, R., McLeod, C. P., Miller, B. A., & New, R. 1998, MNRAS, 298, L7

Chaplin, W. J., Houdek, G., Appourchaux, T., Elsworth, Y., New, R., & Toutain, T. 2008, A&A, 485, 813. 0804.4371

Chaplin, W. J., Houdek, G., Elsworth, Y., Gough, D. O., Isaak, G. R., & New, R. 2005, MNRAS, 360, 859

Chaplin, W. J., Kjeldsen, H., Christensen-Dalsgaard, J., Basu, S., Miglio, A., Appourchaux, T., Bedding, T. R., Elsworth, Y., García, R. A., Gilliland, R. L., Girardi, L., Houdek, G., Karoff, C., Kawaler, S. D., Metcalfe, T. S., Molenda-Żakowicz, J., Monteiro, M. J. P. F. G., Thompson, M. J., Verner, G. A., Ballot, J., Bonanno, A., Brandão, I. M., Broomhall, A.-M., Bruntt, H., Campante, T. L., Corsaro, E., Creevey, O. L., Doğan, G., Esch, L., Gai, N., Gaulme, P., Hale, S. J., Handberg, R., Hekker, S., Huber, D., Jiménez, A., Mathur, S., Mazumdar, A., Mosser, B., New, R., Pinsonneault, M. H., Pricopi, D., Quirion, P.-O., Régulo, C., Salabert, D., Serenelli, A. M., Silva Aguirre, V., Sousa, S. G., Stello, D., Stevens, I. R., Suran, M. D., Uytterhoeven, K., White, T. R.,

- Borucki, W. J., Brown, T. M., Jenkins, J. M., Kinemuchi, K., Van Cleve, J., & Klaus, T. C. 2011, Science, 332, 213. 1109.4723
- Chaplin, W. J., & Miglio, A. 2013, ArXiv e-prints. 1303.1957
- Christensen-Dalsgaard, J. 2011, ADIPLS: Aarhus Adiabatic Oscillation Package (ADIPACK). Astrophysics Source Code Library, 1109.002
- 2012, Astronomische Nachrichten, 333, 914. 1211.2697
- Cox, J. P. 1974, Reports on Progress in Physics, 37, 563
- 1980, Theory of stellar pulsation
- Cox, J. P., & Giuli, R. T. 1968, Principles of stellar structure
- Deheuvels, S., & Michel, E. 2011, A&A, 535, A91. 1109.1191
- Gough, D. O. 1990, in Progress of Seismology of the Sun and Stars, edited by Y. Osaki, & H. Shibahashi, vol. 367 of Lecture Notes in Physics, Berlin Springer Verlag, 283
- Goupil, M. J., Lebreton, Y., Marques, J. P., Deheuvels, S., Benomar, O., & Provost, J. 2011a, Journal of Physics Conference Series, 271, 012032. 1102.0252
- Goupil, M. J., Lebreton, Y., Marques, J. P., Samadi, R., & Baudin, F. 2011b, Journal of Physics Conference Series, 271, 012031. 1102.0247
- Grigahcène, A., Dupret, M.-A., Gabriel, M., Garrido, R., & Scuffaire, R. 2005, A&A, 434, 1055 Hansen, C. J., & Kawaler, S. D. 1994, Stellar Interiors. Physical Principles, Structure, and Evolution.
- Hekker, S., Elsworth, Y., Basu, S., Mazumdar, A., Silva Aguirre, V., & Chaplin, W. J. 2013, ArXiv e-prints. 1306.4323
- Huber, D., Ireland, M. J., Bedding, T. R., Brandão, I. M., Piau, L., Maestro, V., White, T. R., Bruntt, H., Casagrande, L., Molenda-Żakowicz, J., Silva Aguirre, V., Sousa, S. G., Barclay, T., Burke, C. J., Chaplin, W. J., Christensen-Dalsgaard, J., Cunha, M. S., De Ridder, J., Farrington, C. D., Frasca, A., García, R. A., Gilliland, R. L., Goldfinger, P. J., Hekker, S., Kawaler, S. D., Kjeldsen, H., McAlister, H. A., Metcalfe, T. S., Miglio, A., Monteiro, M. J. P. F. G., Pinsonneault, M. H., Schaefer, G. H., Stello, D., Stumpe, M. C., Sturmann, J., Sturmann, L., ten Brummelaar, T. A., Thompson, M. J., Turner, N., & Uytterhoeven, K. 2012, ArXiv e-prints. 1210.0012
- Kippenhahn, R., & Weigert, A. 1990, Stellar Structure and Evolution
- Kjeldsen, H., & Bedding, T. R. 1995, A&A, 293, 87. arXiv:astro-ph/9403015
- Libbrecht, K. G. 1988, ApJ, 334, 510
- Ludwig, H.-G., Caffau, E., Steffen, M., Freytag, B., Bonifacio, P., & Kučinskas, A. 2009, Memorie della Società Astronomica Italiana, 80, 711. 0908.4496
- Marques, J. P., Goupil, M. J., Lebreton, Y., Talon, S., Palacios, A., Belkacem, K., Ouazzani, R.-M., Mosser, B., Moya, A., Morel, P., Pichon, B., Mathis, S., Zahn, J.-P., Turck-Chièze, S., & Nghiem, P. A. P. 2013, A&A, 549, A74. 1211.1271
- Mathur, S., Hekker, S., Trampedach, R., Ballot, J., Kallinger, T., Buzasi, D., García, R. A., Huber, D., Jiménez, A., Mosser, B., Bedding, T. R., Elsworth, Y., Régulo, C., Stello, D., Chaplin, W. J., De Ridder, J., Hale, S. J., Kinemuchi, K., Kjeldsen, H., Mullally, F., & Thompson, S. E. 2011, ApJ, 741, 119. 1109.1194
- Michel, E., Baglin, A., Auvergne, M., Catala, C., Samadi, R., Baudin, F., Appourchaux, T., Barban, C., Weiss, W. W., Berthomieu, G., Boumier, P., Dupret, M.-A., Garcia, R. A., Fridlund, M., Garrido, R., Goupil, M.-J., Kjeldsen, H., Lebreton, Y., Mosser, B., Grotsch-Noels, A., Janot-Pacheco, E., Provost, J., Roxburgh, I. W., Thoul, A., Toutain, T., Tiphène, D., Turck-Chieze, S., Vauclair, S. D., Vauclair, G. P., Aerts, C., Alecian, G., Ballot, J., Charpinet, S., Hubert, A.-M., Lignières, F., Mathias, P., Monteiro, M. J. P. F. G., Neiner, C., Poretti, E., Renan de Medeiros, J., Ribas, I., Rieutord, M. L., Cortés, T. R., & Zwintz, K. 2008, Science, 322, 558. 0812.1267
- Miglio, A. 2012, Asteroseismology of Red Giants as a Tool for Studying Stellar Populations: First Steps, 11
- Miglio, A., Brogaard, K., Stello, D., Chaplin, W. J., D'Antona, F., Montalbán, J., Basu, S., Bressan, A., Grundahl, F., Pinsonneault, M., Serenelli, A. M., Elsworth, Y., Hekker, S., Kallinger, T., Mosser, B., Ventura, P., Bonanno, A., Noels, A., Silva Aguirre, V., Szabo, R., Li, J., McCauliff, S., Middour, C. K., & Kjeldsen, H. 2012, MNRAS, 419, 2077.

- 1109.4376
- Montalbán, J., Miglio, A., Noels, A., Scuflaire, R., Ventura, P., & D'Antona, F. 2012, Adiabatic Solar-Like Oscillations in Red Giant Stars, 23
- Montalbán, J., & Noels, A. 2013, in European Physical Journal Web of Conferences, vol. 43 of European Physical Journal Web of Conferences, 3002
- Mosser, B., Dziembowski, W. A., Belkacem, K., Goupil, M. J., Michel, E., Samadi, R., Soszynski, I., Vrard, M., Elsworth, Y., Hekker, S., & Mathur, S. 2013a, submitted to A&AA&A
- Mosser, B., Elsworth, Y., Hekker, S., Huber, D., Kallinger, T., Mathur, S., Belkacem, K., Goupil, M. J., Samadi, R., Barban, C., Bedding, T. R., Chaplin, W. J., García, R. A., Stello, D., De Ridder, J., Middour, C. K., Morris, R. L., & Quintana, E. V. 2012, A&A, 537, A30. 1110.0980
- Mosser, B., Michel, E., Belkacem, K., Goupil, M. J., Baglin, A., Barban, C., Provost, J., Samadi, R., Auvergne, M., & Catala, C. 2013b, A&A, 550, A126. 1212.1687
- Pamyatnykh, A. A. 1999, Acta Astron., 49, 119
- Pesnell, W. D. 1983, Ph.D. thesis, Florida Univ., Gainesville.
- Samadi, R., Belkacem, K., Ludwig, H.-G., Caffau, E., Campante, T. L., Davies, G. R., Kallinger, T., Lund, M. N., Mosser, B., Baglin, A., Mathur, S., & Garcia, R. A. 2013, submitted to A&A
- Silva Aguirre, V., Casagrande, L., Basu, S., Campante, T. L., Chaplin, W. J., Huber, D., Miglio, A., Serenelli, A. M., Ballot, J., Bedding, T. R., Christensen-Dalsgaard, J., Creevey, O. L., Elsworth, Y., García, R. A., Gilliland, R. L., Hekker, S., Kjeldsen, H., Mathur, S., Metcalfe, T. S., Monteiro, M. J. P. F. G., Mosser, B., Pinsonneault, M. H., Stello, D., Weiss, A., Tenenbaum, P., Twicken, J. D., & Uddin, K. 2012, ApJ, 757, 99. 1208.6294
  Stello, D., Chaplin, W. J., Basu, S., Elsworth, Y., & Bedding, T. R. 2009, MNRAS, 400, L80.
- Tassoul, M. 1980, ApJS, 43, 469

0909.5193

- Tremblay, P.-E., Ludwig, H.-G., Freytag, B., Steffen, M., & Caffau, E. 2013, accepted in A&A Ulrich, R. K. 1986, ApJ, 306, L37
- White, T. R., Bedding, T. R., Stello, D., Christensen-Dalsgaard, J., Huber, D., & Kjeldsen, H. 2011, ApJ, 743, 161. 1109.3455